Mutagenesis of Photosystem I in the Region of the Ferredoxin Cross-Linking Site: Modifications of Positively Charged Amino Acids

Jonathan Hanley, Pierre Sétif, Hervé Bottin, and Bernard Lagoutte*

Département de Biologie Cellulaire et Moléculaire, CEA-Service de Bioénergétique/CNRS-URA 1290, C. E. de Saclay, 91191 Gif sur Yvette Cedex, France

Received February 20, 1996; Revised Manuscript Received April 30, 1996[⊗]

ABSTRACT: The *psa*D gene isolated from the cyanobacterium *Synechocystis* sp. PCC 6803 has been mutated in the region encoding a cross-linking site for ferredoxin. A glucose tolerant strain of *Synechocystis* 6803 was first deleted for *psa*D, and the resulting PS-I was characterised by EPR and flash absorption spectroscopy. The major modification related to the absence of the PsaD subunit is the disappearance of the first order reduction of ferredoxin which is replaced by a second order reaction. Reconstitution of the deleted PS-I with the purified PsaD polypeptide restored 80% of the fast photoreduction of ferredoxin. The deletion of PsaD has no apparent effect on the main biochemical features of the resulting depleted PS-I complex, with the exception of minor modifications to the F_A/F_B centers. The deleted strain was transformed by a series of *psa*D genes mutated at three conserved residues, all located close to the ferredoxin cross-linking site. The resulting photosystem I complexes were extensively studied by flash absorption spectroscopy. Unexpectedly, the change of Lys 106 involved in the cross-linking of ferredoxin for an uncharged amino acid has almost no effect (mutation K106A). However, the functional consequences of more drastic substitutions of either Lys 106 or Arg 111 indicate a role for these two basic amino acids in the binding and submicrosecond reduction of ferredoxin. Various mutations of the unique His at position 97 show that this amino acid is involved in the increased affinity of PS-I for ferredoxin when the pH is lowered. This histidine could be central in regulating *in vivo* the rate of ferredoxin reduction as a precise sensor of the local proton concentration.

Photosystem I is a large multisubunit pigment/protein complex of approximately 300 kDa embedded in the photosynthetic membrane. It comprises at least 11 different subunits and about 100 chlorophyll molecules (Golbeck & Bryant, 1991). The general function of PS-I is that of a light-driven plastocyanin/ferredoxin oxidoreductase. In some organisms, and under certain growth conditions, plastocyanin and ferredoxin can be replaced by a cytochrome c_6 (Ho & Krogmann, 1984) and a flavodoxin (Rogers, 1987), respectively. The redox components involved in the first steps of photoinduced electron transfer are located in the reaction center core complex which is largely hydrophobic and comprises subunits PsaA and PsaB. Light excitation induces charge separation between the primary donor (a dimer of chlorophyll *a* molecules known as P700) and the primary acceptor chlorophyll *a* (A_0). Electron transfer then continues through a series of bound redox cofactors to the terminal acceptors (F_A and F_B), two [4Fe-4S] clusters bound to the peripheral polypeptide PsaC, which is tightly associated to the core complex. Electron transfer then proceeds from F_A and/or F_B to soluble ferredoxin.

The three-dimensional structure of PS-I of the cyanobacterium *Synechococcus elongatus* has been determined at low resolution (Krauss *et al*., 1993). The complex appears to be mostly embedded in the photosynthetic membrane, but there are several important peripheral subunits which protrude into the aqueous environment on the cytoplasmic side of the membrane. Two of these subunits, PsaD and PsaE, have been proposed as candidates for the binding and orientation of soluble ferredoxin to PS-I. The accessibility of PsaD and PsaE to the stromal environment was previously clearly demonstrated by electron microscopy, proteolysis studies, and epitope mapping (Ortiz *et al*., 1985; Lagoutte & Vallon, 1992; Zilber & Malkin, 1992). PsaD was the first subunit to be proposed as the main docking site for ferredoxin on the basis of different cross-linking experiments using EDC (Zanetti & Meratti, 1987; Zilber & Malkin, 1988). In addition to this biochemical approach, the deletion of the corresponding gene in the cyanobacterium *Synechocystis* sp. PCC 6803 was reported to dramatically affect the growth of the modified strain, in agreement with a central role of this polypeptide (Chitnis *et al*., 1989). More recently, the ferredoxin-mediated $NADP^+$ photoreduction was also shown to be considerably impaired in another *psa*D-deleted mutant (Xu *et al*., 1994c). The detailed study of a functional, cross-linked complex between ferredoxin and PS-I allowed identification of Lys 106 (PsaD) and Glu 93 (ferredoxin) as two amino acids involved in the electrostatic interaction between PsaD and ferredoxin (Lelong *et al*., 1994). In addition, it was demonstrated by EPR spectroscopy that the cross-linked ferredoxin was entirely photoreducible, and recent flash absorption studies indicate that the cross-linked complex retains wild type first-order ferredoxin reduction kinetics

* To whom correspondence should be addressed.

[⊗] Abstract published in *Advance ACS Abstracts,* June 15, 1996.

[1] Abbreviations: β-DM, *n*-dodecyl β-D-maltoside; Chl, chlorophyll; DPIP, (2,6-dichlorophenol)indophenol; EDC, *N*-ethyl-3-[3-(dimethylamino)propyl]carbodiimide; EPR, electron paramagnetic resonance; PS-I, photosystem I; F_A, F_B, and F_X, the three [4Fe-4S] centers of PS-I; Fd, ferredoxin; FNR, ferredoxin−$NADP^+$ reductase; HEPES, *N*-(2-hydroxyethyl)piperazine-*N*′-2-ethanesulfonic acid; K_d, dissociation constant; MES, 2-(*N*-morpholino)ethanesulfonic acid; MOPS, 3-(*N*-morpholino)propanesulfonic acid; PsaA, -B, -C, ..., the polypeptides coded by the genes *psa*A, -B, -C, ..., respectively; Tricine, *N*-[2-hydroxy-1,1-bis(hydroxymethyl)ethyl]glycine.

S0006-2960(96)00399-6 CCC: $12.00

(Lelong *et al*., 1996). The sequence around Lys 106 in PsaD was also shown to be probably exposed to the solvent (Xu *et al*., 1994b).

The kinetics of ferredoxin reduction by PS-I have been recently reported, mostly with PS-I and ferredoxin purified from the cyanobacterium *Synechocystis* sp. PCC 6803 (Sétif & Bottin, 1994, 1995). The effects of different ferredoxin mutations on its reduction by PS-I have also been recently reported (Navarro *et al*., 1995). In the present work, we have studied in more detail the consequences of *psa*D deletion on ferredoxin reduction. We have also used site-directed mutagenesis to genetically modify some amino acids in the vicinity of Lys 106 in the PsaD subunit. This allowed further investigation of the nature of the interactions between soluble ferredoxin and the PS-I reaction center of the cyanobacterium *Synechocystis* 6803 and the electron transfer process between these two proteins.

EXPERIMENTAL PROCEDURES

Materials. Most of the molecular biology reagents and enzymes were supplied by Pharmacia, New England Biolabs, and Boehringer Mannheim. The digoxigenin labeling kit and the fluorescent reagent 4-methoxy-4-(3′′-phosphoryloxy)-phenyl-1,2-dioxetane-3-spiro-2′-adamantane (AMPPD) were from Boerhinger Mannheim. Site-directed mutagenesis was carried out following the BioRad kit procedure using the *Escherichia coli* strain CJ 236. Chloramphenicol resistance gene (cam^r) was isolated from plasmid pLF8, a gift from Dr. F. Chauvat (Labarre *et al*., 1989), providing a 1252 bp resistance cassette (Cm^r). The kanamycin resistance gene (kan^r) was from transposon Tn 903 (Pharmacia) and used as a 1300 bp resistance cassette (Km^r). Anti-mouse antibody coupled to alkaline phosphatase was supplied by Promega Biotech, and poly(vinylidene difluoride) (PVDF) membrane for protein transfer was from Millipore. [^{35}S]dATP for sequencing was supplied by Amersham. All other standard chemicals were purchased from Sigma or Merck. All DNA sequences were analyzed using the DNA Strider software (Marck, 1988).

Genetic Constructions. A DNA fragment of 1680 bp was obtained after PCR amplification on the basis of the previously published flanking sequences of the *psa*D gene in *Synechocystis* 6803 (Reilly *et al*. 1988). Unique restriction sites for *Eco*RI and *Bam*HI were introduced respectively at the upstream and downstream ends of the DNA fragment using the PCR primers. This allowed easy subcloning of the fragment into a Bluescript SK+ plasmid (Stratagene) (Figure 1). The cloned *psa*D gene was completely sequenced, including approximately 200 bp of each flanking sequence. This Bluescript construct, BS*psa*D, was then further engineered in order to gain a plasmid aimed at deleting the *psa*D gene in the cyanobacterium (Figure 1, procedure 1). After a restriction step at the unique *Bst*EII and *Hpa*I sites (64 bp upstream and 324 bp downstream of the starting ATG, respectively), the new free ends were blunt ended and ligated to the *Hin*cII Km^r cassette from transposon Tn 903 (Pharmacia). The lengths of the remaining flanking sequences of *Synechocystis* 6803 were of 665 and 627 bp. The latter downstream sequence still included 102 bp of the 3′ end of the *psa*D gene. The resulting plasmid used for *psa*D deletion was named pFBsKD. A second construct was designed to reintroduce the site-mutated *psa*D gene in the deleted *Synechocystis* strain (Figure 1, procedure 2). The *Eco*RI/*Bam*HI fragment was first transferred from BlueScript to M13mp19, and a unique *Sma*I site was created 54 bp downstream of the coding sequence. After the plasmid was restricted at this new site, a Cm^r cassette was introduced, thus leaving the full *psa*D coding sequence unaffected (MJCD). Three fragments of the cyanobacterial DNA are still homologous in the two constructs (dashed upper lined), but recombination events between both types of DNA are most likely to occur in the two larger outside flanking sequences (665 and 471 bp).

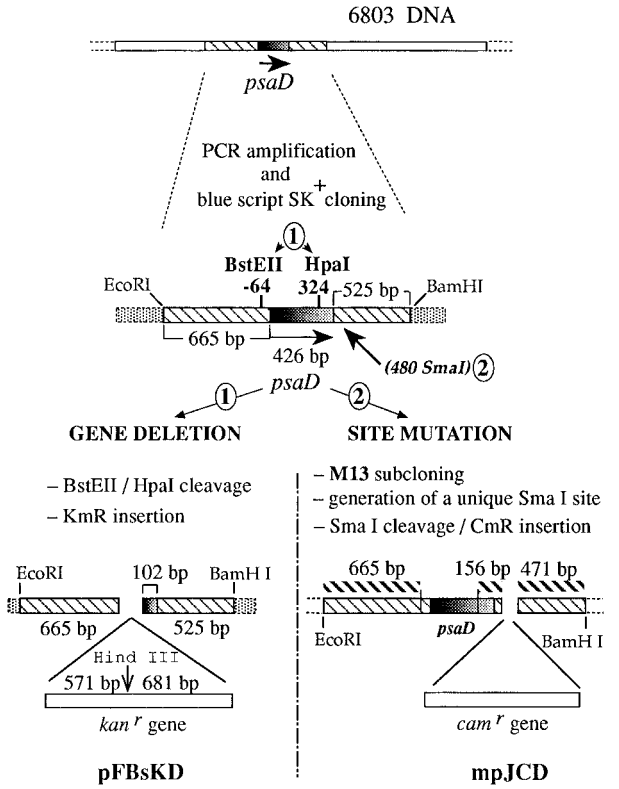

FIGURE 1: Genetic constructions of the two plasmids for *psa*D deletion and *psa*D site-directed mutagenesis. (1) Plasmid pFBsKD was obtained by *Bst*EII/*Hpa*I digestion of *psa*D and replacement of the original *psa*D gene by a Km^r cassette. (2) Plasmid mpJCD was created by transferring the *Eco*RI/*Bam*HI fragment in M13mp19, engineering a unique *Sma*I site 54 bp downstream of *psa*D, and inserting a Cm^r cassette at this new restriction site.

Culture Conditions. Liquid cultures of wild type and mutant cells were grown in BG11 medium (Rippka *et al*., 1979), buffered with 6 mM HEPES (pH 7.3). Solid cultures were on 1.5% agar plates, and HEPES buffer was omitted from BG11. Transformation (Chauvat *et al*., 1986) was carried out either with plasmidic DNA from the Bluescript construct pFBsKD or with the double-stranded M13 MJCD DNA. The growth of liquid cultures was monitored by measuring the optical density at 730 nm and the chlorophyll concentration estimated by the method described in Williams (1988).

In order to delete *psa*D, wild type *Synechocystis* 6803 was first grown under low-light conditions (2.8 μmol m^{-2} s^{-1}) on progressively increasing amounts of glucose, up to 10 mM. The glucose tolerant strain was then deleted of *psaD* using the plasmid pFBsKD. BG11 (50 mL) was inoculated to an OD of 0.2 (730 nm) with wild type cells from a culture in the exponential phase of growth and, then grown to an OD of 1.0. After two washes with fresh culture medium,

the cells were resuspended in 5 mL of the same medium and 1 μg of transformant DNA was added. Transformation proceeded for up to 4 h at 34 °C, under illumination (2.8 μmol m^{-2} s^{-1}). After the transformation incubation, 100 μL aliquots of the cell suspension were spread directly on 5 mM glucose agar plates and allowed to grow for 24 h under very low-light conditions (0.24 μmol m^{-2} s^{-1}); direct light was shielded by four layers of filter paper. Transformant selection was then started by establishing an antibiotic gradient through the agar; the agar plates were incubated at 30 °C under the same very low light (0.24 μmol m^{-2} s^{-1}). The first green colonies were detected after 4−6 weeks. Successive rounds of selection were carried out on 5 mM glucose plates, increasing the kanamycin concentration up to 50 μg/mL, and then further selected through rounds of liquid culture under 0.24 μmol m^{-2} s^{-1} illumination and a constant kanamycin concentration of 50 μg/mL.

One *psa*D-deleted strain, labeled KDb3, was used to raise site-directed mutants of PsaD. Site-directed mutants were generated by direct transformation of the KDb3 with the MJCD M13 constructs and grown for a 24 h period in liquid BG11 and 5 mM glucose. Selection of transformants was carried out by serial dilution in the presence of increasing chloramphenicol concentrations (from 1 up to 30 μg/mL) and decreasing glucose concentrations. Once resistance to 30 μg/mL chloramphenicol was established, the selection procedure was continued through a further 8−10 rounds of liquid subculture.

Genomic DNA Analysis. Genomic DNA from liquid cultures of *Synechocystis* sp. PCC 6803 was isolated as previously described (Tandeau de Marsac *et al*., 1982). Southern hybridization was performed using 2 μg of DNA for each restriction digestion. DNA fragments were electrophoresed on 0.8% agarose gels and transferred to a hybond-N membrane (Amersham) using a vacuum transfer system. The *Eco*RI/*Bam*HI *psa*D insert of the bluescript BS*psa*D plasmid was used as a template for random priming with the digoxigenin dUTP analogue (Boehringer). The resulting labeled mixture was directly used as a probe, following the recommended luminescent detection procedure (Boehringer).

The deletion of the *psa*D gene was monitored by Southern blot analysis. The DNA from KDb3, the selected PsaD-deleted strain, was restricted with either *Hin*dIII or *Hin*cII and then probed with the digoxigenin-labeled *psa*D fragments. With both enzyme cleavages, the original hybridizing fragments present in the wild type were completely replaced by the new fragments expected from the replacement of *psa*D by transposon Tn 903, verifying the homozygosity of the selected strain (data not shown).

Direct Sequencing of PCR-Amplified Genomic DNA. Genomic DNA isolated as above was also used for control sequencing of the mutants. A 524 bp fragment encompassing the full *psa*D sequence was amplified using the PCR procedure with two primers located 58 bp upstream and 39 bp downstream of the coding sequence. A total reaction volume of 100 μL was used, including 0.1−1 μg of genomic DNA, the four dNTPs (0.8 mM), 4 mM $MgCl_2$, and both primers at a concentration of 2.5 μM. Taq polymerase buffer was from Biolabs, and 2.5 u of Ampli Taq (Perkin-Elmer Cetus) was added after a first denaturation step (3 min at 94 °C). Amplification was performed over 35 cycles, each including 1 min of hybridization at 40 °C, 1 min of elongation at 72 °C and 1 min of denaturation at 94 °C. Under these conditions, about 0.5 μg of *psa*D gene was commonly recovered after the electrophoretic purification step. Between 0.1 and 0.2 μg of this double-stranded DNA was used directly for sequencing. Sequencing reactions were carried out by the dideoxy termination method (Sanger *et al*., 1977) using the Pharmacia T7 sequencing kit, after an alkaline denaturation step (Chen & Seeburg, 1985).

Biological Samples. Ferredoxin was isolated from *Synechocystis* sp. PCC 6803 and purified according to Bottin and Lagoutte (1992). Unless otherwise specified, thylakoid membranes were obtained from French press broken cells after extensive washing with ice cold 20 mM Tricine, 10 mM KCl, and 1 mM EDTA (pH 7.8). PS-I was obtained after solubilization with 1% (w/v) β-DM and purified on a sucrose density gradient as described by Rögner *et al*. (1990). The upper green band, consisting of highly enriched monomeric PS-I particles, was dialyzed against 20 mM Tricine/NaOH (pH 7.8) and 0.04% β-DM and concentrated by ultrafiltration (Centriprep 100 instrument, Amicon). The particles were stored at −80 °C. The chlorophyll concentration was determined in 80% Acetone Arnon (1949). The P700 content was calculated from photoinduced absorption changes at 820 nm assuming an absorption coefficient of 6500 M^{-1} cm^{-1} for $P700^+$ (Mathis & Sétif, 1981). The chlorophyll to P700 ratios were thus found to be between 80 and 90 for the different types of isolated PS-I reaction centers, and between 103 and 110 for thylakoid membranes.

Reconstitution of the PsaD-deleted PS-I was carried out using the homologous PsaD polypeptide extracted and purified on the basis of Lagoutte and Vallon (1992). Reconstitution was carried out during 1 h at room temperature by mixing the two components at pH 5.8, with a 10-fold molar excess of PsaD over PS-I. The sample was then dialyzed to pH 7.8 (20 mM Tricine and 0.03% β-DM) overnight at 4 °C, and the excess unbound PsaD subunit was washed away by several rounds of dilution and concentration through a Centriprep 100 concentrator (Amicon).

Antibodies directed against PsaD and PsaE subunits from *Synechocystis* 6803 were obtained as previously described (Rousseau *et al*., 1993) and used at a dilution of 1/200 for immunoblot analysis. Rabbit antibodies against PsaC, a gift from Dr. J. Golbeck, were used at the same dilution. An alkaline phosphatase anti-mouse (or anti-rabbit) conjugate (Promega) was used to reveal the binding of the primary antibody (Lagoutte & Vallon, 1992).

Electrophoresis. Electrophoretic protein characterization was performed using the BioRad mini-slab gel apparatus and the previously described electrophoretic conditions (Lelong *et al*., 1994). Samples were adjusted to 1% SDS and then precipitated for 1 h at −20 °C in 80% acetone. The resulting pellet was resolubilized in the sample buffer described by Laemmli (1970). For antibody probing, gels were transferred electrophoretically on PVDF membranes (Immobilon P from Millipore) as described elsewhere (Lagoutte & Vallon, 1992).

Flash-Absorption Spectroscopy. Laser flash-induced absorption changes at 296 K were measured at 820 nm for P700 and at 580 nm to follow the reduction of ferredoxin, as described previously (Sétif & Bottin, 1994, 1995). Kinetics of ferredoxin reduction are obtained by subtracting the kinetics observed in samples with and without ferredoxin. This subtraction procedure also removes the absorption decay of triplet state antenna pigments (in the microsecond range)

which interfere with the absorption changes due to ferredoxin reduction (Sétif & Bottin, 1994).

EPR. Low-temperature EPR measurements were performed at 10 K with a Bruker ER 200 X-band spectrometer equipped with an Oxford Instruments cryostat. The PS-I particles from the PsaD-deleted mutant were put into calibrated quartz tubes at a chlorophyll concentration of 1 mg/mL. To observe the effect of the absence of PsaD on (F_A, F_B), the samples were poised at pH 8 (50 mM Tricine/NaOH) in the presence of 5 mM sodium ascorbate and 30 mM DPIP. They were then either illuminated at room temperature for 2 min (≈200 mW/cm^2 of white light) before freezing under illumination or dark adapted for 30 min and frozen in the dark. Illumination of dark-adapted samples was subsequently carried out in the cryostat at 10 K.

RESULTS

Characterization of the PsaD-Deleted Mutant

General Characterization. The *psa*D-deleted strain (KDb3) was still able to grow in the absence of glucose at low light intensity (2.8 μmol m^{-2} s^{-1}) under subculturing conditions. The growth rate was approximately 50% of that observed for the same strain in the presence of 5 mM glucose. Increasing the light intensity to 16.8 μmol m^{-2} s^{-1}, in the absence of glucose, further impeded the growth rate to 50% of that observed at a 2.8 μmol m^{-2} s^{-1} light intensity. However, increasing the light intensity from 2.8 to 16.8 μmol m^{-2} s^{-1} in the presence of glucose stimulated growth by 30%.

In addition to the genomic DNA analysis, immunoblotting confirmed the complete absence of any immunologically related PsaD polypeptide in the purified PS-I particles from KDb3 (data not shown). Interestingly, immunoblotting with antibodies specific to PsaC and PsaE demonstrated that these two polypeptides are still incorporated into the membrane in the absence of PsaD and remain bound throughout the PS-I isolation procedure. The presence of a functional PsaC, and the state of the associated (F_A, F_B) clusters, were more accurately analyzed by low-temperature EPR and flash absorption kinetic measurements (see below). In accordance with previous reports, no PS-I trimers were isolated from this deleted mutant after solubilization and purification with β-DM; this procedure normally yields 20% PS-I trimers with the wild type strain. As previously suggested, this indicates either a direct role for PsaD in trimerization or, more likely, an indirect role due to its involvement in the stabilization of PsaL (Chitnis & Chitnis, 1993; Xu *et al*., 1994a).

Electron Paramagnetic Resonance Spectroscopy (EPR). EPR spectra of the iron−sulfur centers (F_A, F_B) were measured in membranes and isolated PS-I prepared from the wild type mutant lacking PsaD; the same results were obtained with both preparations. Figure 2 shows the spectra of PS-I samples prepared in the presence of ascorbate and DPIP at pH 8.0 measured after different illumination conditions. The peak at $g = 1.96$ visible after room-temperature illumination of the sample suggests that (F_A, F_B) are not completely in their native state (Hiyama *et al*., 1984) (panels C and D of Figure 2). Illumination at 10 K of dark-adapted wild type PS-I from *Synechocystis* 6803 induces a single electron transfer to F_A, giving rise to an EPR spectrum with peaks at $g = 2.05$, 1.94, and 1.86 (Figure 2A) (Evans *et al*., 1972; Guigliarelli *et al*., 1992). However, in the mutant lacking PsaD, g values of 2.07, 1.92, and 1.87 are observed which are more typical of F_B^- (Figure 2B). The g value of 1.87 is not typical for F_B^- but may indicate slight line broadening. Illumination at room temperature and freezing under illumination (Figure 2D) results in spectra with major peaks at $g = 2.05$, 1.96, 1.94, 1.92, and 1.89. This is consistent with the reduction of both F_A and F_B, as observed in the wild type (Figure 2C), but the relative intensity of the peaks at 1.94 and 1.89 is lower than generally observed.

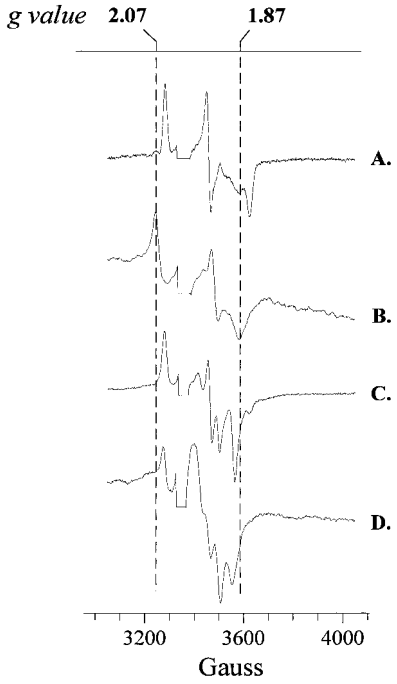

FIGURE 2: EPR spectra of PsaD-deleted PS-I monomers at a concentration of 1 mg/mL in 50 mM Tricine (pH 8.0), 20 μM DPIP, and 10 mM ascorbate. All measurements were made at 10 K using the following instrument settings: microwave power, 20 mW; microwave frequency, 9.426 GHz; and modulation amplitude, 10 G: (trace A) wild type sample dark adapted and then illuminated at 10 K in the EPR cavity, (trace B) PsaD-deleted sample dark adapted and then illuminated at 10 K in the EPR cavity, (trace C) wild type sample illuminated for 2 min at room temperature before freezing, under illumination, at 77 K, and (trace D) PsaD-deleted sample illuminated for 2 min at room temperature before freezing, under illumination, at 77 K.

The preferential photoreduction of F_B at low temperatures has already been reported when core PS-I (without PsaC, PsaD, and PsaE) is reconstituted with PsaC only (Li *et al*., 1991). These authors reported a considerable broadening of the EPR signals ascribed to F_A and F_B in the absence of PsaD followed by narrowing of the EPR lines after reconstitution with PsaD. A significant broadening is not observed in our PS-I preparation from the PsaD-less mutant. This indicates that the absence of PsaD is not sufficient for broadening the EPR signals of (F_A, F_B), the broadening observed by Li *et al*. (1991) possibly being due to a more drastic perturbation resulting from the extraction treatment.

Flash-Absorption Spectroscopy. In wild type control PS-I, light excitation at room temperature results in a charge separation between $P700^+$ and the terminal acceptor, either F_A or F_B. In the absence of forward electron transfer, this is followed by a charge recombination from one of these two centers to $P700^+$, a back-reaction occurring in tens of milliseconds [see Rousseau *et al*., (1993)]. This latter process

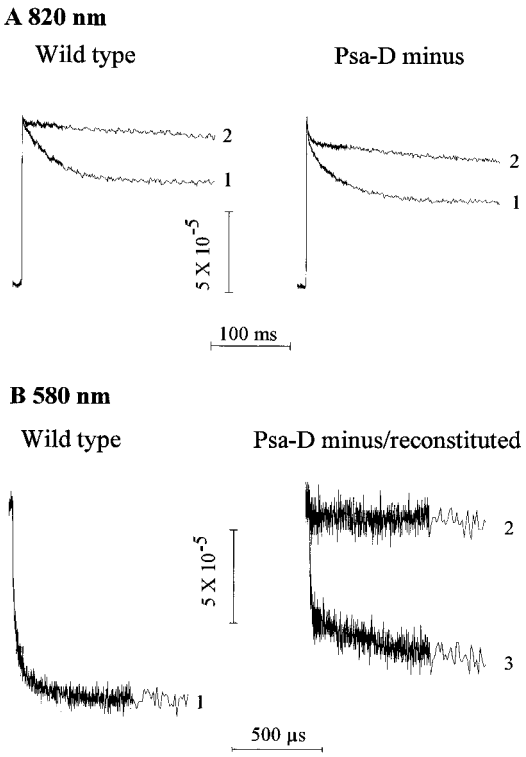

FIGURE 3: Flash absorption measurements in the wild type PS-I, PsaD minus, and PsaD minus reconstituted with PsaD polypeptide. (A) Flash-induced absorption changes at 820 nm of PS-I monomers from wild type and PsaD-deleted *Synechocystis* 6803. For all curves, the PS-I reaction centers were suspended at a P700 concentration of 0.15 μM in 20 mM Tricine (pH 8) in the presence of 0.03% β-DM, 30 mM NaCl, 5 mM $MgCl_2$, 6 μM DPIP, and 1 mM sodium ascorbate: (1) no ferredoxin added and (2) ferredoxin added to a concentration of 2 μM. Traces are the average of eight experiments taken at 10 s time intervals. (B) Kinetics of ferredoxin reduction observed at 580 nm in wild type and PsaD-deleted PS-I obtained by subtracting kinetics in the presence of ferredoxin from kinetics in the absence of ferredoxin: (1) wild type PS-I, (2) PsaD-deleted mutant, and (3) PsaD-deleted mutant reconstituted with isolated PsaD subunit. The PS-I reaction centers were suspended at a P700 concentration of 0.15 μM in 20 mM Tricine (pH 8) in the presence of 0.03% β-DM, 30 mM NaCl, 5 mM $MgCl_2$, 6 μM DPIP, and 1 mM sodium ascorbate. For kinetics measured in the presence of ferredoxin, a final ferredoxin concentration of 1 μM was used. The P700 concentration was verified in each case by measuring the photoinduced absorption change at 820 nm. The kinetics were measured under identical conditions and are thus directly comparable.

can be observed by monitoring the decay of $P700^+$ at 820 nm (Figure 3A, left curve 1).

Addition of soluble ferredoxin leads to a much slower decay of $P700^+$ as electron transfer proceeds now from $(F_A, F_B)^-$ to ferredoxin, and $P700^+$ is then reduced much more slowly by the exogenous donor-reduced DPIP (Figure 3A, left curve). Using a PsaD-depleted PS-I in the absence of ferredoxin, there are two decay components of $P700^+$ due to back-reactions with $t_{1/2}$ of $\approx$1 ms and of tens of milliseconds. There is also a faster component in the microsecond time scale, but this transient is most probably due to triplet states of antenna chlorophylls, as it is no longer observable when using subsaturating laser intensities. After subtraction of these antenna signals from the original decay curves, there remains a component of $t_{1/2}$ of $\approx$1 ms which accounts for approximately 10% of the total decay (Figure 3A, right curve 1). The low-temperature EPR data presented in this work indicate that the vast majority of (F_A, F_B) centers are intact in the PsaD-less PS-I, but the slight changes in the EPR spectra outlined above reflect a low level of (F_A, F_B) degradation. The 1 ms decay observed at 820 nm could be ascribed to a recombination between F_X^- and $P700^+$ in this small proportion of altered centers (Golbeck & Cornelius, 1986). In the presence of ferredoxin, the decay of $P700^+$ becomes slower, indicating that PsaD-deleted PS-I is still capable of some forward electron transfer in the presence of soluble ferredoxin (Figure 3A, right curve 2). The 1 ms transient is still present, independent of the addition of ferredoxin, showing that charge recombination between $P700^+$ and F_X^- is preferred to the forward electron transfer from F_X to ferredoxin.

In a second series of experiments, we directly monitored the reduction of soluble ferredoxin by PS-I, on the basis of the previously described differential absorption between reduced [2Fe-2S] and [4Fe-4S] clusters. Sétif and Bottin (1994, 1995) analyzed the reduction of ferredoxin by wild type PS-I at pH 8.0 in the presence of 5 mM $MgCl_2$ and 30 mM NaCl. They characterized a complex reduction process, with three first-order components of $t_{1/2} \approx 500$ ns, 20 μs, and 100 μs (see Figure 3B, curve 1, and Figure 5A, left curve). The dissociation constant (K_d) of the complex was calculated to lie between 0.40 and 0.60 μM, the saturation of the signal amplitude being reached at about 2 μM Fd for a 0.2 μM concentration of P700. The kinetics of ferredoxin reduction were also studied at pH 5.8 in the absence of salts. At this lower pH, the affinity of PS-I for ferredoxin is much higher than at pH 8.0 ($K_d \approx 0.05$ μM), and the kinetics of ferredoxin reduction are much faster (a major submicrosecond phase and a single first-order microsecond phase with $t_{1/2} \approx 9$ μs), with a 100 μs first-order phase being essentially absent (see Figure 5A and Table 1). At pH 5.8, there is also no requirement for salts. In the PsaD-deleted mutant, the first-order kinetics are no longer observed up to a ferredoxin concentration of 8 μM (Figure 3B, curve 2). This indicates an affinity decrease of more than 16-fold as compared to that of the wild type. A second-order slow phase of reduction is observable. but the rate of this process is so slow that the reduction of ferredoxin is obscured by reoxidation. Only an upper limit for the second-order rate constant can be calculated, $k_2 < 0.5 \times 10^8$ M^{-1} s^{-1}. We tentatively tried to restore the normal kinetics of ferredoxin by adding the purified PsaD subunit to the deleted PS-I particle, in a way similar to the previously described recovery of ferredoxin reduction kinetics on reconstitution of PsaE (Rousseau *et al*., 1993). Following reassociation of PsaD, it was possible to observe recovery in the signal amplitude of ferredoxin reduction. Using saturating amounts of ferredoxin, the recovery corresponds to 80% of the reduction amplitude observed in the wild type (Figure 3B, curve 3). The missing 20% can be attributable to modified PS-I as a result of some alteration of (F_A, F_B) centers, destabilization of PsaE, or due to a fraction of incorrectly reassociated PsaD. The dissociation constant of the reconstituted system was not measured precisely, but it can be deduced, from the amplitude of the signal shown in Figure 3, that it is slightly smaller than 1 μM.

Site-Directed Mutagenesis of PsaD

Lys 106 and Arg 111 are two conserved basic residues in the PsaD sequence at, or near, the ferredoxin cross-linking site (Lelong *et al.*, 1984). These positively charged residues

Table 1: Properties of Ferredoxin Reduction in Wild Type and Site-Directed Mutants of PsaD

strain	experimental conditions	no. of first-order phases ($t_{1/2}$)	% of each phase of first-order reduction (580 nm)	K_d (μM)
WT 6803	pH 8.0, salts[a]	3	<1 μs	40	0.4−0.6[b]
			13 μs	38	
			85 μs	23	
	pH 5.8, no salts	2	<1 μs	46	0.05
			9 μs	54	
psaD H97E	pH 8.0, salts	2 (3)	<1 μs	29	3,8
			(24 μs)	(4)	
			111 μs	67	
	pH 5.8, no salts	0		–	–
	pH 5.8, salts	3	<1 μs	22	0.3
			16 μs	32	
			<150 μs	46	
psaD H97N	pH 8.0, salts	3	<1 μs	37	0.8
			16 μs	34	
			135 μs	29	
	pH 5.8, no salts	2	<1 μs	25	0.5
			9 μs	76	
psaD H97K	pH 8.0, salts	3	<1 μs	42	0.7
			14 μs	40	
			80 μs	18	
	pH 5.8, no salts	2	<1 μs	45	0.25
			10 μs	55	
psaD K106A	pH 8.0, salts	3	<1 μs	42	0.8
			15 μs	28	
			86 μs	30	
	pH 5.8, no salts	2	<1 μs	48	≈0.07
			9 μs	52	
psaD K106C	pH 8.0, salts	3	<1 μs	33	2.2
			20 μs	34	
			120 μs	33	
	pH 5.8, no salts	2 (3)	<1 μs	30	
			10 μs	64	0.7
			(110 μs)	(6)	
psaD R111C	pH 8.0, salts	3	<1 μs	18	1.8
			15 μs	27	
			120 μs	55	
	pH 5.8, no salts	2 or 3	<1 μs	20	
			9 μs	68	0.6
			80 μs	12	

[a] In the whole table, salts refers to a final concentration of 5 mM $MgCl_2$ and 30 mM NaCl. [b] Two limits instead of a mean value are given for the wild type, according to the previously reported measurements by Sétif and Bottin (1994).

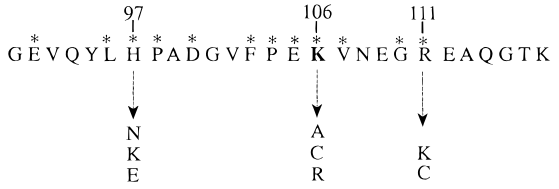

FIGURE 4: Amino acid sequence of *Synechocystis* 6803 PsaD close to the previously identified cross-linking site (K106) between PsaD and ferredoxin. The stars (*) denote the conserved residues in this region. All point mutations discussed in this paper are shown below the wild type sequence.

were obvious targets in a search for impairing the interaction between PS-I and the acidic ferredoxin. A series of site-directed mutants were obtained for each of these residues (Figure 4); the results of the most interesting mutations on the different reduction parameters of ferredoxin are summarized in Table 1. From this table, it can be seen that the replacement of the basic Lys 106 residue by a neutral alanine has little effect on the kinetics of ferredoxin reduction at pH 8.0. There are three first-order phases with half-times similar to the wild type values, and the dissociation constant is only slightly increased to 0.8 μM (vs 0.4−0.6 μM). The kinetics at pH 5.8 are also very close to those observed in the wild type, with the presence of two fast phases (<1 and 10 μs) and the 100 μs phase being essentially absent. A similar increase in affinity for ferredoxin is also observed when going from pH 8.0 to 5.8.

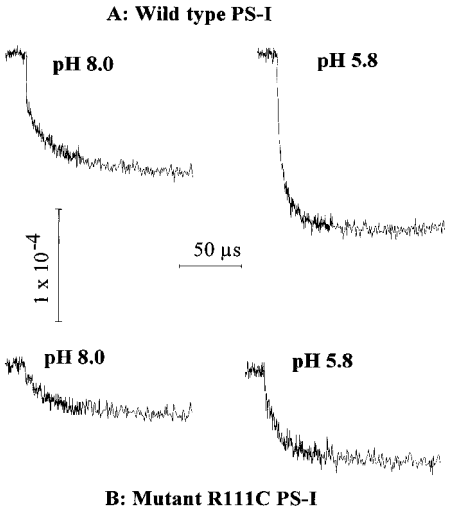

FIGURE 5: Kinetics of ferredoxin reduction observed at 580 nm in wild type and mutant R111C obtained by subtracting kinetics measured in the presence and absence of ferredoxin: (A) wild type PS-I, (B) mutant R111C measured, (left column) pH 8.0, and (right column) pH 5.8. The PS-I reaction centers were suspended at a P700 concentration of 0.15 μM in either 20 mM Tricine (pH 8) 0.03% β-DM, 30 mM NaCl, 5 mM $MgCl_2$, 6 μM DPIP, and 1 mM sodium ascorbate or 20 mM MES (pH 5.8), 0.03% β-DM, 120 μM DPIP, and 5 mM sodium ascorbate. For kinetics measured in the presence of ferredoxin, a final concentration of 1 μM ferredoxin was used.

More interesting effects were observed when either Lys 106 or Arg 111 was replaced by cysteine. Measurements of ferredoxin reduction at pH 8.0 by PS-I from mutant R111C in the presence of salts indicate an apparent 3−4 fold decrease in affinity for ferredoxin ($K_d \approx 1.8$ μM). In mutant K106C, the affinity for ferredoxin is further reduced, with $K_d \approx 2.2$ μM. Three different first-order phases were observed in both cases, but a comparison of their relative amplitudes indicates that the first-order reduction process is slower than that observed in the wild type. Decreasing the pH to 5.8 results in a slight increase in affinity ($K_d \approx 0.6$−0.7 μM), but this value is still far from the reported K_d of 0.05 μM for the wild type at the same pH. The rate of reduction is slightly increased at pH 5.8 but is still slower than in the wild type. Preliminary data suggest that using a more acidic pH further increases the ferredoxin affinity in mutants K106C and R111C, together with some substantial increase in the amplitude of the submicrosecond phase of reduction. These more acidic conditions, which are probably nonphysiological, induce no noticeable modifications in the interaction between ferredoxin and PS-I in the wild type or mutant K106A. The reintroduction of a different basic residue at either position 106 or 111 restored a K_d at pH 8.0 very close to the wild type value. This was achieved by an arginine substitution at position 106 (K106R), giving a K_d of 0.8 μM, or a lysine substitution at position 111 (R111K), with a resulting K_d of 0.7 μM. Any small differences in K_d

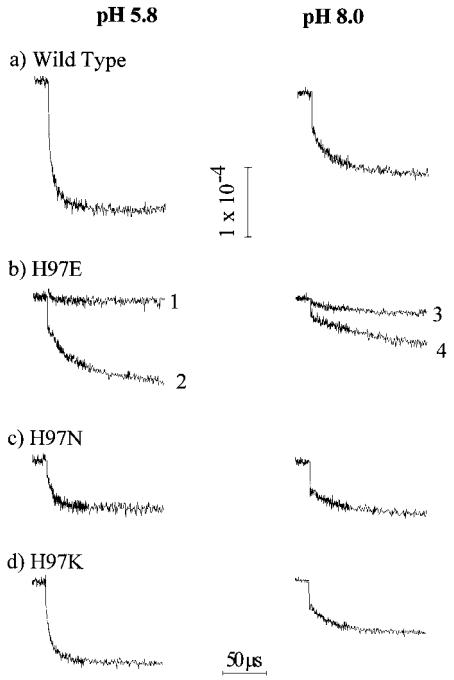

FIGURE 6: Kinetics of ferredoxin reduction observed at 580 nm in wild type and the three H97 mutants (E, N, and K) obtained at pH 5.8 (left column; 20 mM Mes, 120 μM DPIP, and 5 mM sodium ascorbate; no salts except curve b2, 5 mM $MgCl_2$) or pH 8.0 (right column; 20 mM Tricine, 30 mM NaCl, 5 mM $MgCl_2$, 6 μM DPIP, and 1 mM sodium ascorbate). A final concentration of 1 μM ferredoxin was used for obtaining all curves, except curve b4 (5 μM ferredoxin).

may arise from the differences in the length of the side chains between arginine and lysine, without important consequences on the general charge pattern required at this site.

The results of the wild type PS-I characterization demonstrate that pH modifications induce changes at three different levels: the affinity of PS-I for ferredoxin, the relative amplitudes of first-order phases of ferredoxin reduction, and the alteration of the salt requirement. At pH 8.0, a salt concentration of 5 mM $MgCl_2$ and 30 mM NaCl is used in order to gain optimum ferredoxin binding. However, at pH 5.8, divalent or monovalent ions are not required for ferredoxin binding. This suggests that there may be a protonation of one or more residues at pH 5.8 which are unprotonated at pH 8.0. The pH effect observed between pH 5.8 and 8.0 prompted us to modify His 97, a residue not far from the cross-linking site which could potentially be protonated in this pH range. The greatest effect was seen in mutant H97E. In this mutant, the photoreduction of ferredoxin strictly required the presence of $MgCl_2$ at pH 5.8 as well as at pH 8.0. In the absence of $MgCl_2$, using a ferredoxin concentration of 5 μM, all first-order reduction is completely lost (Figure 6b, trace 1). In the case of this particular mutant, the divalent cation requirement is vital and cannot be fulfilled by the addition of high NaCl concentrations. It is important to note that, in the presence of $MgCl_2$, there are three first-order components present with $t_{1/2} < 1$ μs, ≈ 10 μs, and ≥ 150 μs. This again differs greatly from the situation in the wild type where only two components of $t_{1/2} < 1$ and 9 μs are observed at pH 5.8. At pH 8.0, in the presence of $MgCl_2$, there is a 6−8-fold decrease in the affinity and the 10 μs phase of reduction is essentially lost, being replaced by a large 110 μs phase which forms 65−70% of the total first-order reduction (Table 1).

Replacement of histidine 97 by asparagine (H97N), a neutral residue, has little effect on the reduction of ferredoxin when it is measured at pH 8.0 in the presence of salts. The proportions of each kinetic phase are similar to those of the wild type, although there is a small increase in K_d to 0.8 μM which accounts for the difference in the overall amplitude of the kinetic trace (Figure 6c). A larger difference between this mutant and wild type PS-I becomes apparent when ferredoxin reduction is measured at pH 5.8 in the absence of salts. The expected disappearance of the slower phase is observed; however the proportion of the 10 μs phase is higher, and the relative increase in affinity for ferredoxin is not as large as that observed in the wild type (Table 1 and Figure 6c). Replacing His 97 with a basic lysine residue (H97K) almost completely rescued the wild type reduction kinetics. There is a normal salt requirement at pH 8.0, and the K_d is 0.7 μM. There are three phases of reduction present, with $t_{1/2} < 1$, 13. and 80 μs, and the relative amplitudes of these phases are similar to those observed in the wild type (Figure 6d and Table 1). At pH 5.8, there is no salt requirement, the 100 μs phase is absent, and the proportions of the two first-order phases are now similar to those of the wild type (Figure 6d). An increase in affinity for ferredoxin is clearly observed, but not as large as that for the wild type.

DISCUSSION

A general role for PsaD in the $NADP^+$ reduction via ferredoxin has been reported (Xu *et al.*, 1994c), but no precise function was reported in the reduction of ferredoxin itself. We demonstrate in this work the direct requirement of PsaD to observe first-order reduction of ferredoxin, the fast processes being no longer observed in the deleted mutant up to a ferredoxin concentration of 8 μM (0.2 μM PS-I). The second-order rate of reduction is also reduced by at least 1 order of magnitude in the PsaD-less mutant. However, analysis of the $P700^+$ decay following single-flash excitation indicates that there is little back-reaction between $F_{(A/B)}^-$ and $P700^+$. This may indicate that the slower ferredoxin reduction process does not prevent a relatively large yield of reduced ferredoxin. In agreement with this *in vitro* observation, the slower reduction of ferredoxin still supports a photosynthetic growth of the deleted strain in the absence of glucose, provided a low light intensity is used (2.8 μmol m^{-2} s^{-1}). It has been reported that the PsaD-less strain barely grows in the absence of glucose (Xu *et al.*, 1994); however, a light intensity of 21 μmol m^{-2} s^{-1} was used during these experiments. It has been demonstrated here that at such high light intensities the growth rate of PsaD-less 6803 is markedly impaired. This is difficult to interpret, but it has been reported that the absence of PsaD probably induces a high turn over of PS-I peripheral polypeptides (Chitnis & Nelson, 1992). The expected consequence *in vivo* is a generally lower proportion of "functional" PS-I, thus impairing the electron transfer to ferredoxin with increased light intensity. Alternatively, it is possible that the use of low light (2.8 μmol m^{-2} s^{-1}) prevents some photoinhibition events which inhibit growth at higher light intensities.

The absence of PsaD in a deleted mutant of the same strain was reported to modify the peripheral polypeptide content of the purified PS-I (Chitnis *et al.*, 1989). In contradiction with these findings, immunoblot analysis performed on the PsaD-deleted strain used in the present work revealed that

PsaC and PsaE are still present in both membranes and β-DM-purified PS-I complex. Reconstitution experiments also clearly demonstrated that a major fraction of these two subunits is functionally associated to this PS-I. Indeed, reconstitution of the purified PsaD subunit to the deleted system allowed an 80% recovery of the fast first-order reduction of ferredoxin. Such a result could not be obtained in the absence of a large fraction of PsaE, as it has been previously demonstrated that PsaE is also essential for obtaining a fast ferredoxin reduction (Rousseau *et al.*, 1993). The present work thus corroborates in a functional way a recent report on the quantitative presence of PsaE in another PsaD-less mutant of *Synechocystis* 6803 (Xu *et al*., 1994a).

Previous experiments indicated a role of the PsaD subunit in the stabilization of PsaC, the polypeptide bearing the terminal acceptors F_A and F_B (Li *et al.*, 1991). However, in the results reported here, there seems to be little change in the stability of PsaC in the absence of PsaD. We confirm the preferential photoreduction of F_B at low temperatures in the absence of PsaD (Li *et al.*, 1991), but there is no significant broadening of the EPR line shapes. The discrepancy between both works may be explained by the severe treatment used for the biochemical extraction and reconstitution experiments. The purification of the reconstituted PS-I was also carried out on Triton X-100. whereas in all the data reported here, β-DM was used throughout. It is possible that Triton X-100 is a more disruptive detergent. Alternatively, we may have selected suppressor mutation, together with the deletion of PsaD, which partly compensates the destabilization effect promoted by the absence of PsaD. However, a number of *psa*D minus strains were selected, all of which had the same genotypic and phenotypic characteristics. It is unlikely that all of the selected strains would contain the same suppressor which stabilizes PsaC.

To characterize further the residues of PsaD which could be important in the ferredoxin/PS-I interaction, we studied some site mutations aimed at modifying the conserved positive charges located close to Lys 106. An unexpected result was the almost silent effect of the alanine substitution of lysine 106 at the cross linking site. This could be tentatively explained assuming that the site for the correct binding and orientation of ferredoxin is made of a multiple charge frame. The change in binding energy when a single positive charge is deleted may therefore be of small magnitude. This multiple charge frame could involve, among others, Arg 111 and His 97. The neutral substitution of just one of these residues thus has a minimal effect, as observed for K106A, the K_d and the optimum orientation of ferredoxin being achieved by the remaining residues. Replacement of Lys 106 or Arg 111 by Cys has a more disruptive effect on the ferredoxin/PS-I interaction. The results indicate that, in these two mutants, at pH 8.0, the first-order reduction occurs at a slower rate and the affinity for ferredoxin is decreased. Lowering the pH at 5.8 increases both the affinity for ferredoxin and the rate of the first-order reduction, but the dissociation constant is still much higher than that for the wild type PS-I. Considering that the K106A mutant behaves like the wild type, it appears likely that the main perturbation brought about by the cysteine mutations could be the presence of an additional group which remains negatively charged between pH 5.8 and 8.0, thus leading to some electrostatic repulsion with acidic groups of ferredoxin. At both locations (C106 and C111), the immediate environment must considerably lower the pK_a of the thiol group, which normally titrates around 8.5 for free cystein. However, this unexpected effect is not strong enough to abolish the full set of interactions with other accessible basic residues in PsaD. We thus suggest that Lys 106 and Arg 111 are present within the binding site, but each alone plays only a small role in the global affinity of PS-I for ferredoxin.

Characterization of wild type ferredoxin reduction has shown that at pH 5.8 the first-order rate of ferredoxin reduction and its affinity for PS-I increase as compared to those at pH 8.0. This suggests that at least one residue could be protonated between pH 8.0 and 5.8, enhancing the interaction between PS-I and soluble ferredoxin. A more efficient reduction of ferredoxin can also be achieved at pH 8.0 by the addition of divalent cations, indicating that the role of the proposed protonation may be partially compensated for by the presence of divalent cations at the higher pH. One obvious candidate responsible for this pH effect could be His 97, the single highly conserved histidine in PsaD. It is not far from the cross-linked Lys 106 in the primary sequence, and the mean pK_a of the imido group ($\approx$6) can fit the range of the pH effect. Substitution of His 97 for Glu results in a strict requirement for $MgCl_2$ to obtain a first-order reduction, even at pH 5.8. This shows that His 97 is probably an essential part of the ferredoxin binding site in the tertiary structure of PsaD, in a crucial place for the binding regulation of ferredoxin. This unexpected requirement for $MgCl_2$ at pH 5.8 in H97E indicates that a salt bridge could be present between this new Glu 97 in PsaD and an acidic residue in ferredoxin.

Our results suggest that there is little difference between mutant H97N and the wild type at pH 8.0. At pH 5.8, the same increase in the rate of ferredoxin reduction is observed, but not the 10-fold increment in affinity. This loss of pH dependent affinity suggests that His 97 is at least partially responsible for the pH effect in the wild type. Replacing His 97 by Lys results in reduction kinetics similar to those of the wild type PS-I when they are measured at both pH 5.8 and 8.0. From Table 1. it can be seen that the relative amplitude of the submicrosecond phase increases from 25% in H97N to 45% in H97K, thus indicating a faster ferredoxin reduction in H97K. However, in this last mutant, the full extent of the pH effect regarding the affinity increase at low pH is not observed ($K_d \approx 0.25$ μM instead of 0.05 μM). This cannot be explained by an electrostatic effect and rather suggests that the longer side chain of Lys 97 may sterically hinder the PS-I/ferredoxin interaction.

From this last set of mutations, the unique histidine of PsaD appears to be a good candidate to explain the increased affinity and rate of reduction of ferredoxin at low pH. This residue could act as a precise sensor to accelerate the ferredoxin reduction in relation to a transient acidification of the PS-I acceptor side, a possible situation in the case of an increased proton flow through the ATPase. However, when histidine is replaced by a neutral amino acid, there is still some increase in the affinity and rate of ferredoxin reduction at the lower pH. It is thus likely that other residues are also involved in this important pH effect which is currently the subject of further investigation.

The presence of three different first-order phases during the reduction of ferredoxin by PS-I led to the proposed existence of well-separated ferredoxin binding sites, with F_A being the partner of ferredoxin in one site and F_B in the other

(Sétif & Bottin, 1994, 1995). Within such a model, it is expected that site mutations may disrupt preferentially one site versus the other, thus leading to an almost complete disappearance of at least one first-order component, but conserving the other components. Such an effect was not clearly observed for any of the mutations described in the present study, despite the fact that a significant decrease in the global affinity of ferredoxin for PS-I was detected in several cases. There are some modifications in the proportions of the different first-order phases for mutants K106C and R111C, and a considerable increase in the amplitude of the slower first-order phase is also observed for mutant H97E. These modifications may suggest the existence of two overlapping binding sites. However, from the present results, it appears that an increase in affinity of ferredoxin for PS-I is generally correlated with an increase in the proportion of the fastest submicrosecond phase. When another model to explain the kinetic complexity of ferredoxin reduction is being sought, it is tempting to assign the fastest component to a PS-I/ferredoxin complex in which the relative orientations of ferredoxin and PS-I would be optimal for electron transfer. In this interpretation, the slowest component could be ascribed to a less favorable binding of ferredoxin, possibly in the same PS-I region responsible for the optimal complex. However, the spectral differences between the intermediate and slow phases are difficult to understand within such a model. It appears therefore that the reason for the existence of at least three different first-order phases remains, for the moment, unexplained.

ACKNOWLEDGMENT

We are very grateful to Dr. Francoise Rousseau for providing the *psa*D PCR fragment and the Blue Script construct for deleting the *psa*D gene and to Fraser MacMillan for EPR spectroscopy.

REFERENCES

Arnon, D. I. (1949) *Plant Physiol. 24*, 1−15.
Bottin, H., & Lagoutte, B. (1992) *Biochim. Biophys. Acta 1101*, 48−56.
Chauvat, F., De Vries, L., Van der Ende, A., & Van Arkel, G. A. (1986) *Mol. Gen. Genet. 204*, 185−191.
Chauvat, F., Rouet, P., Bottin, H., & Boussac, A. (1989) *Mol. Gen. Genet. 216*, 51−59.
Chen, E. J., & Seeburg, P. H. (1985) *DNA 4*, 165−170.
Chitnis, P. R., & Nelson, N. (1992) *Plant Physiol. 99*, 239−246.
Chitnis, P. R., Reilly, P. A., & Nelson, N. (1989) *J. Biol. Chem. 264*, 18381−18385.
Chitnis, V. P., & Chitnis P. R. (1993) *FEBS Lett. 336*, 330−334.
Evans, M. C. W., Telfer, A., & Lord, A. V. (1972) *Biochim. Biophys. Acta 267*, 530−537.
Golbeck, J. H., & Cornelius, J. M. (1986) *Biochim. Biophys. Acta 849*, 16−24.
Golbeck, J. H., & Bryant, D. A. (1991) in *Current Topics in Bioenergetics (Govindjee, Ed.)* pp 83−177, Academic Press, London.
Guigliarelli, B., Guillaussier, J., More, C., Sétif, P., Bottin, H., & Bertrand, P. (1993) *J. Biol. Chem. 264*, 900−908.
Hiyama, T., Ohtsuka, T., & Sakurai, H. (1984) *J. Biochem. 95*, 855−860.
Ho, K. K., & Krogmann, D. W. (1984) *Biochim. Biophys. Acta 766*, 310−316.
Krauss, N., Hinrichs, W., Witt, I., Fromme, P., Pritzkow, W., Dauter, Z., Betzel, C., Wilson, K. S., Witt, H. T., & Saenger, W. (1993) *Nature 361*, 326−330.
Labarre, J., Chauvat, F., & Thuriaux, P. (1989) *J. Bacteriol. 171*, 3449−3457.
Laemmli, U. K. (1970) *Nature 227*, 680−685.
Lagoutte, B., & Vallon, O. (1992) *Eur. J. Biochem. 205*, 1175−1185.
Lelong, C., Setif, P., Lagoutte, B., & Bottin, H. (1994) *J. Biol. Chem. 269*, 10034−10039.
Lelong, C., Bœkema, E., Kruip, J., Bottin, H., Rögner, M., & Sétif, P. (1996) *EMBO J.* (in press).
Li, N., Zhao, J., Warren, P. V., Warden, J. T., Bryant, D. A., & Golbeck, J. H. (1991) *Biochemistry 30*, 7863−7872.
Marck, C. (1988) *Nucleic Acids Res. 16*, 1829−1836.
Mathis, P., & Sétif, P. (1981) *Isr. J. Chem. 21*, 316−320.
Navarro, J. A., Hervàs, M., Genzor, C. G., Cheddar, G., Fillat, M. F., de la Rosa, M. A., Gomez-Moreno, C., Cheng, H., Xia, B., Chae, Y. K., Yan, H., Wong, B., Straus, N. A., Markley, J. L., Hurley, J. K., & Tollin, G. (1995) *Arch. Biochem. Biophys. 321*, 229−238.
Ortiz, W., Lam, E., Chollar, S., Munt, D., & Malkin, R. (1985) *Plant Physiol. 77*, 389−397.
Reilly, P. A., Hulmes, J. D., Pan, Y.-C. E., & Nelson, N. (1988) *J. biol. Chem. 263*, 17658−17662.
Rippka, R., Deruelles, J., Waterbury, J. B., Herdmann, M., & Stanier, R. Y. (1979) *J. Gen. Microbiol. 111*, 1−61.
Rogers, L. J. (1987) in *The Cyanobacteria* (Fay, P., & Van Baalen, C., Eds.) pp 35−67, Elsevier, Amsterdam.
Rögner, M., Nixon, P. J., & Diner, B. A. (1990) *J. Biol. Chem. 265*, 6189−6196.
Rousseau, F., Sétif, P., & Lagoutte, B. (1992) *EMBO J. 12*, 1755−1765.
Sanger, F., Nicklen, S., & Coulson, A. R. (1977) *Proc. Natl. Acad. Sci. U.S.A. 74*, 5463−5467.
Sétif, P. Q. Y., & Bottin, H. (1994) *Biochemistry 33*, 8495−8504.
Sétif, P. Q. Y., & Bottin, H. (1995) *Biochemistry 34*, 9059−9070.
Tandeau de Marsac, N., Borrias, W. E., Kuhlemeier, C. J., Castets, A. M., van Arkel, G. A., & van den Hondel, C. A. M. J. J. (1982) *Gene 20*, 111−119.
Williams, J. G. K. (1988) *Methods Enzymol. 167*, 766−778.
Xu, Q., Trent, S., Armbrust, T. S., Guikema, J. A., & Chitnis, P. R. (1994a) *Plant Physiol. 106*, 1057−1063.
Xu, Q., Guikema, J. A., & Chitnis, P. R. (1994b) *Plant Physiol. 106*, 617−624.
Xu, Q., Jung, Y.-S., Chitnis, V. P., Guikema, J. A., Golbeck, J. H., & Chitnis, P. R. (1994c) *J. Biol. Chem., 269*, 21512−21518.
Yu, L., Zhao, J., Lu, W., Bryant, D. A., & Golbeck, J. H. (1993) *Biochemistry 32*, 8251−8258.
Zanetti, G., & Merati, G. (1987) *Eur. J. Biochem. 169*, 143−146.
Zilber, A. L., & Malkin, R. (1988) *Plant Physiol. 88*, 810−814.
Zilber, A. L., & Malkin, R. (1992) *Plant Physiol. 99*, 901−911.

BI960399X